Available online at www.sciencedirect.com
SCIENCE DIRECT®
Nuclear Instruments and Methods in Physics Research A 511 (2003) 347–353
NUCLEAR INSTRUMENTS & METHODS IN PHYSICS RESEARCH Section A
www.elsevier.com/locate/nima

Measurements of muon flux at 1070 m vertical depth in the Boulby underground laboratory

M. Robinson[a,*], V.A. Kudryavtsev[a], R. Lüscher[b], J.E. McMillan[a], P.K. Lightfoot[a], N.J.C. Spooner[a], N.J.T. Smith[c], I. Liubarsky[b]

[a] *Department of Physics and Astronomy, University of Sheffield, Hicks Building, Hounsfield Road, Sheffield S3 7RH, UK*
[b] *Blackett Laboratory, Imperial College of Science, Technology and Medicine, London SW7 2BZ, UK*
[c] *Rutherford Appleton Laboratory, Particle Physics Department, Chilton, Oxon, OX11 0QX, UK*

Received 13 January 2003; received in revised form 12 June 2003; accepted 16 June 2003

Abstract

Measurements of cosmic-ray muon rates and energy deposition spectra in a 1 t liquid scintillator detector at 1070 m vertical depth in the Boulby underground laboratory are discussed. In addition, the simulations used to model the detector are described. The results of the simulations are compared to the experimental data and conclusions given. The muon flux in the laboratory is found to be $(4.09 \pm 0.15) \times 10^{-8}$ cm^{-2} s^{-1}.

PACS: 96.40.Tv; 25.30.M; 95.35

Keywords: Underground muons; Dark matter; Muon flux; Neutron background

1. Introduction

Dark matter Weakly Interacting Massive Particle (WIMP) experiments attempt to identify WIMP-induced events in ultra low background detectors. The dominant backgrounds in such experiments cause electron recoils within the detectors. Techniques such as pulse shape discrimination in a scintillator are used to distinguish between these events and the nuclear recoil events expected from WIMP interactions. Neutron interactions also cause nuclear recoils and are not distinguished from WIMP interactions by these methods. Alternative systems must therefore be used to suppress the neutron background in these experiments.

Neutrons in underground laboratories are primarily due to (α, n) reactions caused by α-decay of U/Th traces in the rock and detector materials. Such neutrons typically have energies of a few mega electron volts. Passive neutron shielding of an appropriate thickness around the detectors may be used to suppress these neutrons, increasing the sensitivity of the experiment.

Neutrons are also produced by muon interactions in the rock and detector materials. These neutrons may have much higher energies, the

*Corresponding author. Tel.: +44-0-114-222-3553; fax: +44-0-114-272-8079.
E-mail address: matthew.robinson@sheffield.ac.uk (M. Robinson).

0168-9002/$ - see front matter
doi:10.1016/S0168-9002(03)01973-9

spectrum extending into the GeV range. Passive neutron shielding is not sufficient to suppress such neutrons.

Muon-induced neutron background may be suppressed using an active muon veto around the detector so that neutrons accompanied by a muon signal in the veto may be rejected. This will be necessary for experiments to achieve sensitivities of less than 10^{-8} pb in terms of WIMP–nucleon interaction cross-section. The design of such vetos will require a good understanding of the energy spectrum and flux of muons passing through the laboratory.

Since the rock density and composition at Boulby are not well known, a direct measurement of the muon flux in the laboratory was performed to provide normalisation to simulations of muon-induced neutrons. A detector normally used as a gamma background veto for the Zoned Proportional Scintillation in Liquid Noble Gases (ZePLiN I) [1] dark matter experiment was used to measure this flux.

In this paper, we will describe the measurements made with the detector. We will also describe the simulations of the muon spectrum in the laboratory and of muon interactions in this detector. Finally, we will discuss the analysis of these data to calculate the muon flux in the experiment and thereby the effective depth of the laboratory for muon suppression in terms of metres of water equivalent.

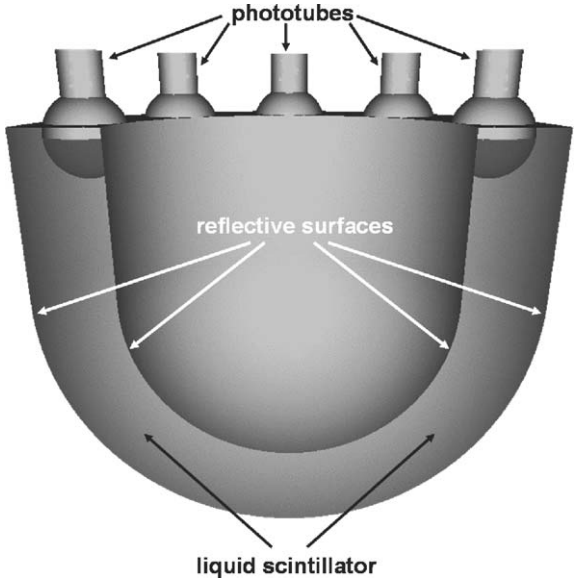

Fig. 1. Cross-sectional diagram of ZePLiN I gamma veto scintillator detector which was used to measure muon rate. The detector has 10 phototubes but only five are shown here.

Table 1
Specifications of liquid scintillator EJ-399-01

Density	0.89 g/cm^3
Wavelength of maximum emission	425 nm
Light output	57% Anthracene
Attenuation length	> 2 m
Flash point	145°C
Average atomic number	4.75
Average atomic mass	8.33

2. Experimental setup

The ZePLiN I veto detector (Fig. 1) is a hollow structure surrounding the main ZePLiN I experiment on five sides. The lower part of the detector is hemispherical in shape with an inner radius of 0.35 m and an outer radius of 0.65 m giving a wall thickness of 0.3 m. The upper part is cylindrical in shape with the same inner and outer radii and a height of 0.6 m. The liquid scintillator within has a mineral oil base containing approximately 25% phenyl-o-xylylethane (PXE) supplied by Eljen Technology under the product name EJ-399-01 (See Table 1 for specifications). This was chosen primarily for its high flash point due to safety constraints on materials used at Boulby. The volume of the detector is 1.05 m^3, giving a total mass of liquid scintillator of 0.93 t. The scintillator is viewed from above by ten 20 cm hemispherical phototubes (Electron tubes [2] model[1] 9354KA). The inside surfaces of the detector are covered in aluminium with a coefficient of reflection greater than 0.9 to maximise light collection.

No specially designed Data Acquisition (DAq) system was used for the muon measurements. Instead, the DAq systems developed for the UK

[1] The model 9354KA PMTs used are standard 9354KB specified for low activity glass.

dark matter searches were used. The UK Dark Matter Collaboration (UKDMC) has recently switched DAq from a system employing digital oscilloscopes read into a G3 Macintosh computer through a General Purpose Interface Bus (GPIB) system using LabView software, to an Acqiris Compact PCI [3] digitiser system read into a PC under custom written Linux software. Both of these systems were used to collect muon data in order to examine possible DAq related systematic errors. Both DAq systems output digitised pulses to binary data files. The pulses stored in the binary files were analysed using custom written data analysis software. The pulses were analysed in terms of amplitude in mV and in terms of integrated area in $\mathrm{mV}\times\mathrm{ns}$. The two analysis methods produced similar results. The dynode chains on the detector PMTs were intended to provide a simple low-level trigger rather than linear energy measurement and show pronounced non-linearity effect for high-amplitude pulses. This effect was quantified by measuring the PMT signal amplitude from fast LED pulses over a range of amplitudes and the muon data were corrected accordingly.

The γ emission lines at 1275 MeV and 1333 MeV from a ^{60}Co were used to collect calibration data for the detector. These data were analysed using the same techniques as for muon data. In addition, the simulations discussed in Section 3 showed a peak at around 60 MeV which also appeared in the data and was used as a calibration point. This peak is due to muons which pass through the bottom part of the detector and, therefore, have a track length inside the detector of 30 cm. These two calibration points were found to agree in terms of the ratio of pulse amplitude to deposited energy.

3. Simulations

The simulation code MUSIC [4] was used to calculate the angular distribution and energy spectrum of muons expected at various depths underground. This was achieved by starting with the muon angular distribution and energy spectrum at sea level and then propagating these muons through either Boulby rock, or standard rock to various depths. The muon energy spectrum at various zenith angles at sea level was taken according to the parameterisation by Gaisser [5], modified for large zenith angles [6] with the best fit values for normalisation and spectral index obtained by the LVD experiment [6,7]. Note that the LVD results also agree with the parameterisation obtained in the MACRO experiment [8]. Standard rock is defined to have atomic number 11, atomic mass 22 and density 2.65 g/cm^3. Geological survey information was supplied by Cleveland Potash Ltd, the operators of the Boulby mine. The average atomic number of Boulby rock was estimated to be 11.7 ± 0.5 and the atomic mass to be 23.6 ± 1.0. The vertical depth of the laboratory was measured as 1070 m and the density was estimated to be 2.70 ± 0.10 g/cm^3. It was found that the muon energy spectrum and mean muon energy at the depth of the Boulby mine laboratory do not depend strongly on either the rock composition or the exact depth.

The detector simulation was performed using custom written C++ code. Five surfaces are simulated to represent the geometry of the detector (Fig. 1). The bottom of the detector is represented by two hemispheres, the top by a hollow disc and, the sides are represented by two cylinders. The phototubes are represented by discs within the hollow disc surface.

Muons are generated on the surface of a 2 m sided cube centred on the origin of the hemisphere surfaces. Muon energy and direction were chosen according to the calculated energy spectrum and angular distribution at a depth of 3000 m of water equivalent in Boulby rock, and the area of the detector perpendicular to the muon flux was taken into account. The assumption that the muon direction is unaffected by interaction with the detector is used throughout the simulation. Once generated, each muon is propagated through the 2 m cube using a ray-tracing algorithm until it passes through one of the five surfaces. Once it has passed through the surface, the muon is considered to be inside the detector. The muon is then propagated again until it passes through another detector surface and is then considered to have left the detector. Propagation of the muon continues

until the ray-tracing algorithm determines that it will not pass through any of the five surfaces again. Due to the geometry of the veto, it is legitimate for the muon to pass through the surfaces zero, two or four times. This is a useful verification employed in the code. Further verification of the performance of the simulation is provided by a GIMP Toolkit (GTk) [9] graphical user interface which uses the same ray-tracing algorithms used in the simulation to draw the veto surfaces, phototube surfaces and muon tracks to the screen. The graphical user interface also serves to confirm that the normals to the surfaces are correctly calculated which is required for light transport (discussed below). The information acquired by propagating the simulated muons is used to calculate the depth of scintillator each muon passed through. This is then used to generate a track length histogram for a suitably large number of simulated muons (Fig. 2a).

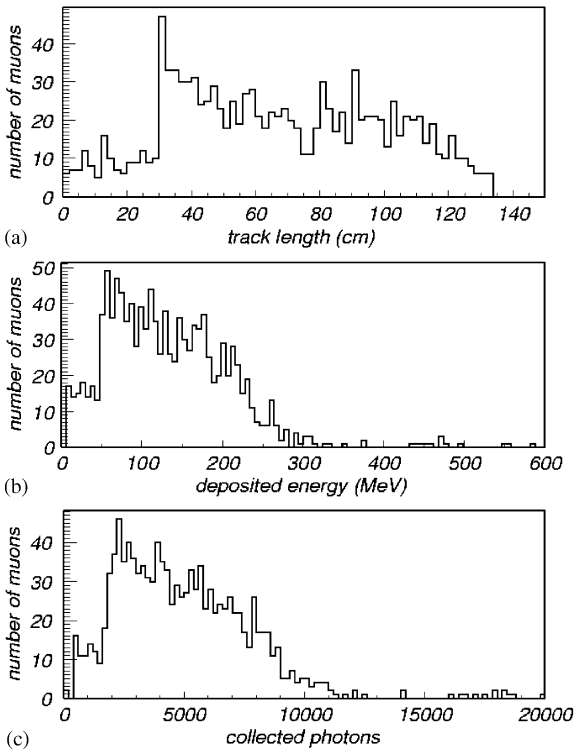

Fig. 2. Histograms of muon track length (a), energy loss (b) and collected photons (c) from simulation of muons passing through the detector.

Since the thickness of the scintillator is small, all processes of muon interaction with matter other than ionisation could be neglected. Muon energy deposition due to ionisation in the detector is sampled from a Landau distribution. The mean energy loss for ionisation and atom excitation is calculated from the muon energy, path length through the scintillator and the properties of the scintillator (Table 1) using the Bethe–Bloch formula [10]. A second histogram was generated showing the distribution of energy deposition (Fig. 2b).

The calculations up to this point were verified by repeating the simulation using the FLUKA [11] code and comparing the distributions of energy deposition.

Due to the position of the phototubes on the detector and the overall detector shape, light collection for light emitted in the bottom of the detector is less efficient than for light emitted in the sides. This is clear from the fact that here is a direct line of sight from the phototubes to the sides of the detector but not to the bottom. In order to account for this, it was necessary for the simulation to also include light transport of the scintillation photons within the detector. Once the energy deposition of each muon has been calculated, that value is converted into a number of photons decided randomly based on a Gaussian distribution. The mean of the Gaussian distribution is calculated from the muon energy deposition and mean scintillation efficiency (Table 1). The square root of the mean is used as the standard deviation of the Gaussian distribution. The initial position of each photon is determined by choosing a random point along the muon track through the veto and the direction is chosen randomly from a uniform solid angle distribution.

Photon transport is handled by repeatedly reflecting each photon from the five detector surfaces until its fate is decided. After photon initialisation and following each reflection, the same ray-tracing algorithms used in muon propagation are used to determine the next surface which the photon will hit. The probability of bulk absorption within the liquid along the path to that surface is calculated based on the scintillator

attenuation length (Table 1) and a random number generated to determine, based on that probability, whether the photon should be considered absorbed. For the purposes of photon reflection, the surfaces are modelled as slightly crumpled metal. To simulate this, the normal to the surface is rotated by a random amount within a limited range. Upon each intercept with a detector surface, the photon is reflected specularly from the surface based on the modified normal to the surface. The probability of photon absorption on the surface is calculated from the reflectance of the surface and a random number is generated to determine whether the photon should be considered absorbed or reflected. This process continues until the photon undergoes absorption on a surface, bulk absorption in the liquid or intercepts the photocathode of a photomultiplier. If the photon intercepts a photocathode before being absorbed, a random number is generated to determine, based on the PMT efficiency (taken as 20%), whether the photon is detected. If a photon intercepts a photocathode and is detected, this is recorded. Any photon hitting a photocathode and not detected is considered to have been absorbed. In this way a histogram of number of detected photons is built up (Fig. 2c) which, with suitable normalisation, may be compared to the measured spectrum.

4. Results

Measurements were taken of the rate of muons depositing 30 MeV or more in the detector over 53 days. The data were taken over three runs, the results of which are given in Table 2.

Table 2
Muon rates in data collection runs

Run start	N_{muons}(E > 30 MeV)	duration (days)	rate (day^{-1})
26-7-02	1028	19.830	51.8 ± 1.6(stat)
28-8-02	712	12.886	55.3 ± 2.1(stat)
11-9-02	1097	20.249	54.2 ± 1.6(stat)
Total	2837	52.965	53.6 ± 1.0(stat)

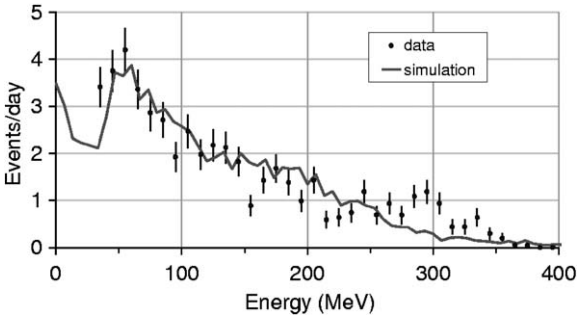

Fig. 3. Muon energy deposition spectrum using data collected in the run starting 11-9-02 (Table 2).

Fig. 3 shows the energy spectrum for the run dated 11th September compared with the normalised simulated spectrum of energy deposition. The spectrum of energy deposition was obtained from the spectrum of collected photons using the calibration peak at around 60 MeV discussed above.

It was possible to use the simulation to calculate the proportion of muons passing through a 2 m sided cube around the veto which can be expected to deposit 30 MeV or more in the detector. These figures were then used to calculate the flux of muons in the laboratory. Eq. (1) gives the effective area $\langle S \rangle$ of a 2 m sided cube normalised by relative muon intensity:

$$\langle S \rangle = \frac{\int I_\mu(\theta,\phi) S_\perp(\theta,\phi) \mathrm{d}\Omega}{\int I_\mu(\theta,\phi) \mathrm{d}\Omega}, \quad (1)$$

where $I_\mu(\theta,\phi)$ is the flux of muons as a function of zenith angle (θ) and azimuthal angle (ϕ) in the laboratory, $S_\perp(\theta,\phi)$ is the area of the 2 m sided cube perpendicular to the muon flux as a function of zenith and azimuthal angle. At the Boulby laboratory depth, this calculation gives an effective area of 58 029 cm^2. The simulations showed that of those muons passing through the 2 m sided cube, a fraction 0.261 ± 0.003(stat) are expected to pass through the detector and deposit 30 MeV or more in the detector. This figure gives an effective area for the detector of 15 146 cm^2. The calculated effective area was found to depend only slightly on the estimate of the vertical depth of the laboratory. Reducing the estimated depth by 200 m w.e., the effective area was calculated as 15 139 cm^2. (Note

that the standard analysis technique involving the evaluation of the detector acceptance as a function of θ and ϕ, described in Refs. [6,8], cannot be applied because the information about the muon directions is not available. The angular bins to be included in the calculation of the acceptance are therefore not known.) Using the total rate from Table 2, the flux is calculated to be $I_\mu = (4.09 \pm 0.08(\text{stat}) \pm 0.13(\text{syst})) \times 10^{-8}$ cm^{-2} s^{-1}. The systematic error is made up of contributions from cuts applied to the measured spectra to remove γ background, contributions from the simulations, uncertainty in the non-linearity correction applied to the data, and uncertainty in the energy calibration of the measured spectrum. Assuming a flat surface, the effective vertical depth of the laboratory in terms of metres of water equivalent was estimated by comparing the calculated muon intensities (see Section 3 for a description of the simulations) with our measurements. Using atomic number 11.7 and atomic mass 23.6 as discussed in Section 3 for Boulby rock, this was calculated as 2805 ± 15 m w.e. based on the measured muon flux. Using atomic number 11 and atomic mass 22 as for standard rock, the effective vertical depth would be 2845 ± 15 m w.e. Based on the difference between the two vertical depth calculations the systematic error on the vertical depth due to incomplete information on the rock composition is estimated to be ± 40 m w.e. The final vertical depth estimate is therefore 2805 ± 45 m w.e. Using the effective vertical depth and the measured depth of the laboratory (1070 m), the mean rock density is calculated as 2.62 ± 0.01 g/cm^3 for Boulby rock and 2.66 ± 0.01 g/cm^3 for standard rock.

For purposes of comparison with other similar measurements, the vertical muon intensity was calculated as

$$I_{\text{vert}} = \frac{N_\mu}{\langle S\Omega \rangle \varepsilon} = 3.32 \times 10^{-8} \text{ cm}^{-2} \text{ sr}^{-1} \text{ s}^{-1}, \quad (2)$$

where I_{vert} is the vertical muon intensity, N_μ is the muon rate in the detector in s^{-1}, $\langle S\Omega \rangle$ is the angular acceptance of the detector in cm^2 sr and ε is the fraction of muons depositing > 30 MeV in the detector calculated in the simulations. The quantity $\langle S\Omega \rangle$ was calculated from the simulations in a similar way to the effective area $\langle S \rangle$ (See Eq. (1)).

5. Conclusions

Muon rate data were collected using the ZePLiN I veto detector in the Boulby mine laboratory. These data were used in conjunction with simulations of the detector and of the muon spectrum to calculate the muon flux in the laboratory.

The muon flux in the laboratory has been measured as $(4.09 \pm 0.15) \times 10^{-8}$ cm^{-2} s^{-1}. This shows an effective vertical depth of 2805 ± 45 m of water equivalent, and a mean rock density of 2.62 ± 0.03 g/cm^3.

These measurements will provide normalisation to neutron flux simulations and help to design muon veto systems for future dark matter experiments.

Acknowledgements

The authors would like to thank the members of the UK Dark Matter Collaboration for their valuable assistance and advice. We are grateful to the Particle Physics and Astronomy Research Council for financial support and to Cleveland Potash Limited for their assistance. M. Robinson would also like to thank Hilger crystals for their support of his Ph.D. work.

References

[1] R. Lüscher, et al., Nucl. Phys. B (Proc. Suppl.) 95 (2001) 233.
[2] http://www.electron-tubes.co.uk/forms/pdf/9354KB.pdf.
[3] http://www.acqiris.com/Products/DC110.html.
[4] P. Antonioli, C. Ghetti, E.V. Korolkova, V.A. Kudryavtsev, G. Sartorelli, Astroparticle Phys. 7 (1997) 357.
[5] T.K. Gausser, Cosmic Rays and Particle Physics, Cambridge University Press, Cambridge, 1990.
[6] LVD Collaboration, M. Aglietta, et al., Phys. Rev. D 58 (1998) 092005.
[7] LVD Collaboration, M. Aglietta, et al., Phys. Rev. D 60 (1999) 112001.

[8] MACRO Collaboration, M. Ambrosio, et al., Phys. Rev. D 52 (1995) 3793.
[9] http://www.gtk.org.
[10] H.A. Bethe, Rev. Mod. Phys. 9 (1937) 69; C. Bloch, Phys. Rev. 93 (1954) 1094.
[11] A. Fassò, A. Ferrari, P.R. Sala, in: A. Kling, F. Barao, M. Nakagawa, L. Tavora, P. Vaz (Eds.), Proceedings of the Monte Carlo 2000 Conference, Lisbon, 23–26 October, 2000, Springer, Berlin, 2001, p. 159;
A. Fassò, A. Ferrari, J. Ranft, P.R. Sala, in: A. Kling, F. Barao, M. Nakagawa, L. Tavora, P. Vaz (Eds.), Proceedings of the Monte Carlo 2000 Conference, Lisbon, 23–26 October, 2000, Springer, Berlin, 2001, p. 995.